

APPLICATION OF ULTRA-NARROWBAND SYSTEMS TO LOW POWER WIDE AREA NETWORKS

A Degree Thesis

Submitted to the Faculty of the

Escola Tècnica Superior d'Enginyeria de Telecomunicació de Barcelona

Universitat Politècnica de Catalunya

By

Marina Alonso Poal

In partial fulfilment of the requirements for the Degree in
Telecommunications Science and Technology Engineering

Advisors

Prof. Ana Isabel Pérez Neira

Dr. Màrius Caus López

Barcelona, June 2017

Abstract

Concepts such as Internet of Things (IoT) or Machine to Machine (M2M) are gaining more and more interest as they will provide connectivity for countless number of devices. The main challenge of this paradigm is to connect these devices at a low cost, with a limited infrastructure and featuring a very long-life time with mild energy requirements.

The goal of the investigation underlying this Degree Thesis is to analyze in detail Ultra Narrow-Band (UNB) systems as a candidate solution for Low Power Wide Area Networks (LPWAN), which are fundamental to support IoT applications.

Firstly, a basic Point to Point (P2P) baseband communication system is simulated, which is later on extended into a passband system. The next step focuses on studying several PHY (abbreviation for Physical Layer) aspects, such as the modulation and the pulse-shaping. From this chapter, it can be concluded that the Differential Binary Phase-Shift Keying (DBPSK) modulation is an excellent option for a UNB communication both for its robustness to the phase offset induced by the channel and its acceptable Bit Error Rate (BER). Concerning the pulse shaping, performance metrics such as the BER, the Power Spectral Density (PSD) and the Peak to Average Power Ratio (PAPR) reveal that the pulse used in Gaussian Minimum Shift Keying (GMSK) with a length of 4 symbol periods, is an excellent option.

Later on, relevant aspects from the Medium Access Control (MAC) layer are studied. In this regard, it has been decided to simulate the ALOHA random access mechanism in its four variants (pure and slotted in time and frequency domains). It is concluded that the hybrid cases where at least pure ALOHA is performed in one domain are the best options to be used in a UNB system. To be able to extend the coverage to places where there is no terrestrial infrastructure, the application of UNB to satellite networks is evaluated. In this case, the analysis is conducted taking advantage of the study carried out in terrestrial environments. It has concluded that UNB systems could deal with the impairments of the satellite, such as the Doppler effect, by properly designing the receiver.

The main contribution of this project to the State of the Art is the conclusion taken from this final part of the thesis, where it is demonstrated that the Doppler effect evaluated on different elevations has not a negative impact on the random-access characteristics, leading to the conclusion that satellite communications are indeed a good option in LPWAN in terms of random access.

Resum

Conceptes com la Internet de les Coses (IoT) o el Màquina a Màquina (M2M) estan guanyant cada cop més i més interès ja que proveiran connectivitat a un incomptable nombre de dispositius. El principal repte d'aquest paradigma és connectar aquests dispositius a un baix cost, amb una infraestructura limitada i que tinguin una vida llarga amb requeriments energètics baixos.

L'objectiu d'aquesta investigació subjacent a aquest Treball de Fi de Grau és estudiar la aplicació de sistemes de banda ultra estreta (UNB) com una solució candidata per a xarxes de llarg abast i de baix consum (LPWAN), claus per a suportar aplicacions de IoT.

Primerament, es simula un sistema de comunicacions punt a punt (P2P) banda base, que després s'estén a un sistema passabanda. El pas següent es centra en estudiar diferents aspectes PHY, com la modulació o els pols conformador. D'aquest capítol es pot concloure que la DBPSK és una opció excel·lent per a les comunicacions UNB tant per la seva robustesa a l'offset de fase introduït pel canal com la seva bona taxa d'error de bit. Respecte el pols conformador, mètriques com la BER, la densitat espectral de potència (PSD) i la relació de pic amb la potència mitja (PAPR), revelen que el pols utilitzat en GMSK amb una longitud de 4 períodes de símbol és una opció excel·lent.

A continuació s'estudien aspectes rellevants de la capa MAC (control d'accés al medi). Per a aquest treball s'ha escollit crear un entorn que simuli el mecanisme d'accés aleatori ALOHA en les seves quatre variants (pur i ranurat en els dominis temps i freqüència). Es conclou que els casos híbrids on com a mínim l'ALOHA pur es dona en un domini són les millors opcions a utilitzar en un sistema UNB. Per a poder estendre la cobertura on no hi ha infraestructura terrestre, s'avalua la opció satèl·lit. En aquest cas, la anàlisi es realitza aprofitant l'estudi desenvolupat per als escenaris terrestres. Es conclou que els sistemes UNB podrien tractar amb els impediments dels satèl·lits tals com l'efecte Doppler, si el receptor es dissenya properament.

La contribució principal d'aquest projecte al State of the Art és la conclusió extreta de la part final de la tesis, on es demostra que l'efecte Doppler avaluat en diferents elevacions no té un impacte negatiu en les característiques d'accés aleatori, arribant a la conclusió de que les comunicacions per satèl·lit són efectivament una bona opció per a LPWAN, en termes d'accés aleatori.

Resumen

Conceptos como el Internet de las Cosas (IoT) o el Máquina a Máquina (M2M) están ganando cada vez más y más interés ya que proveerán conectividad a un incontable número de dispositivos. El principal reto de este paradigma es conectar estos dispositivos a un bajo precio, con una infraestructura limitada y con una larga vida con requerimientos energéticos bajos.

El objetivo de esta investigación subyacente a este Trabajo de Final de Grado es analizar en detalle sistemas de banda estrecha (UNB) como una solución candidata para redes de largo alcance y de bajo consumo (LPWAN), claves para soportar aplicaciones de IoT.

Primeramente, se simula un sistema de comunicaciones banda base punto a punto (P2P) básico que después se extiende a un sistema paso banda. El siguiente paso se centra en estudiar aspectos relevantes de la capa PHY, como la modulación y el pulso conformador. De este capítulo se concluye que la modulación DBPSK es una excelente opción para comunicaciones UNB debido tanto a su robustez frente a offsets en la fase introducidos por el canal como a su buena tasa de error de bit (BER). Respecto al pulso conformador, métricas como la BER, la densidad espectral de potencia (PSD) y la relación de pico a potencia media (PAPR) revelan que el pulso usado en GMSK con una longitud de 4 periodos de símbolo es una excelente opción.

A continuación, aspectos relevantes de la capa MAC se estudian. En este caso, se ha decidido simularse un mecanismo de acceso aleatorio ALOHA en sus cuatro variantes (puro y ranurado para los dominios en tiempo y frecuencia). Se concluye que los casos híbridos donde como mínimo el ALOHA puro se realiza en un dominio son las mejores opciones para un sistema UNB. Para poder extender la cobertura donde no hay infraestructura terrestre, se evalúa la aplicación de UNB a redes satélite. En este caso, se realiza el estudio aprovechando la simulación realizada para ambientes terrestres. Se concluye finalmente que los sistemas UNB pueden tratar con los impedimentos de los satélites, como el efecto Doppler, si se diseña correctamente el receptor.

La contribución principal de este proyecto al State of the Art es la conclusión sacada de la parte final de la tesis, donde se demuestra que el efecto Doppler evaluado en diferentes elevaciones no tiene un impacto negativo en las características del acceso aleatorio, concluyendo así que las comunicaciones por satélite son efectivamente una buena opción para LPWAN, en términos de acceso aleatorio.

Contents

Abstract	1
<i>Resum</i>	2
<i>Resumen</i>	3
List of Acronyms	5
List of Notations	6
List of Figures	7
1 Introduction	8
1.1 Project Outline	8
1.2 Requirements and Specifications	8
1.3 Time Planning	8
1.4 State of the Art	9
2 PHY Layer: Point to Point Communications System	11
2.1 Introduction	11
2.2 P2P	11
2.3 Differential Modulations	13
2.4 Shaping Pulses	15
2.5 Conclusions	20
3 MAC Layer: Random Access Schemes	22
3.1 Introduction	22
3.2 ALOHA Schemes	22
3.3 Satellite Access	26
3.4 Conclusions	30
Conclusions	31
References	32

List of Acronyms

3GPP	3 rd Generation Partnership Project
AMP	Amplitude Modulated Pulse
AWGN	Additive White Gaussian Noise
BER	Bit Error Rate
BPSK	Binary Phase-Shift Keying
CCDF	Complementary Cumulative Distribution Function
CSS	Chirp Spread Spectrum
DBPSK	Differential Binary Phase-Shift Keying
DSSS	Direct Sequence Spread Spectrum
FSTS	Frequency Slotted Time Slotted
FSTU	Frequency Slotted Time Unslotted
FUTS	Frequency Unslotted Time Slotted
FUTU	Frequency Unslotted Time Unslotted
GMSK	Gaussian Minimum-Shift Keying
IOT	Internet Of Things
LEO	Low Earth Orbit
LPWAN	Low-Power Wide-Area Network
MAC	Medium Access Control
MAP	Maximum A Posteriori
MSK	Minimum-Shift Keying
M2M	Machine to Machine
NGSO	Non-Geostationary Satellite Orbit
PAPR	Peak to Average Power Ratio
PHY	Abbreviation for Physical Layer
PSD	Power Spectral Density
P2P	Point to Point
QPSK	Quadrature Phase-Shift Keying
RMS	Root Mean Square
RPMS	Random Phase Multiple Access
SLL	Side Lobe Level
SNR	Signal-to-Noise Ratio
SRRC	Square-Root Raised Cosine
UNB	Ultra-NarrowBand

List of Notations

$\mathbf{a}[\mathbf{k}]$	Random Bits Sequence
$\hat{\mathbf{a}}[\mathbf{k}]$	Estimation of the Random Bits Sequence
$\mathbf{b}[\mathbf{n}]$	Symbols Sequence
$\hat{\mathbf{b}}[\mathbf{n}]$	Estimation of the Symbols Sequence
$\mathbf{b}_s(\mathbf{t})$	Baseband Transmitted Signal
\mathbf{b}	Frequency Slot Duration
\mathbf{B}	Total Frequency Window
\mathbf{f}_d	Doppler Frequency
\mathbf{f}_0	Carrier Frequency
\mathbf{G}	Load of an ALOHA scheme
\mathbf{h}	Satellite Orbit Height
$\mathbf{I}[\mathbf{k}]$	Phase Symbols
\mathbf{n}_{col}	Number of Collided Transmissions
\mathbf{n}_{suc}	Number of Successful Transmissions
\mathbf{n}_{tran}	Number of Total Transmissions
$\mathbf{r}(\mathbf{t})$	Received Signal
\mathbf{R}_E	Radius of the Earth
$\mathbf{s}(\mathbf{t})$	Transmitted Signal
$\mathbf{S}_{\text{PP}}(\mathbf{f})$	Power Spectral Density of a Pulse
\mathbf{S}	Throughput of an ALOHA scheme
\mathbf{T}	Total Time Window
$\mathbf{p}(\mathbf{t})$	Shaping Pulse
$\mathbf{Q}[\mathbf{k}]$	Quadrature Symbols
τ	Temporal Slot Duration
ϑ	Nadir Angle
ω_{sat}	Satellite Angular Velocity

List of Figures

Figure 1	Gantt Diagram of the Time Planning for this project
Figure 2	Scheme of a baseband communications system
Figure 3	Transmitted signal and two received signals with different N_0
Figure 4	Scheme of a passband communications system
Figure 5	Power Spectral Density Estimation of a baseband and a passband signal
Figure 6	Scheme of the ideal DBPSK encoder and decoder
Figure 7	Example of a binary input with its correspondent DBPSK output
Figure 8	BER comparison using different modulations and a SRRC pulse
Figure 9	SRRC temporal representation for different roll-off factor values
Figure 10	Representation of a MSK Pulse of Length = 1
Figure 11	Representation of GMSK Pulses of Length = 1 and Length = 4
Figure 12	BER comparison using different shaping pulses
Figure 13	PSD comparison using different shaping pulses
Figure 14	CCDF comparison using different shaping pulses
Figure 15	Distribution examples of different ALOHA schemes
Figure 16	Throughput comparison of different ALOHA schemes
Figure 17	Collision probability comparison of different ALOHA schemes
Figure 18	Detection probability comparison of different ALOHA schemes
Figure 19	Example of different elevation values in a satellite environment
Figure 20	Distribution example of an unslotted ALOHA in a satellite environment
Figure 21	Collision probability comparison between terrestrial and satellite ALOHA
Figure 22	Detection probability comparison between terrestrial and satellite ALOHA

1 Introduction

1.1 Project Outline

The project is carried out at the Department of Signal Theory and Communications of the Technical University of Catalonia (UPC - BarcelonaTech) in collaboration with the Telecommunications Technological Centre of Catalonia (CTTC).

The goal of the project is to study the application of ultra-narrowband systems to achieve long-range communications with low power consumption. Towards this end, starting from a simple point to point communication system, a multi-user ultra-narrowband communication system will be described.

Once the system model is characterized, different communication channels must be studied with special emphasis to the satellite channel. Hence, the impact of the satellite channel on the MAC procedures, such as the users' access mechanism to the system, are going to be thoroughly studied.

1.2 Requirements and Specifications

This project has been developed following the succeeding requirements.

- The communication system analysis must include the PHY and MAC aspects of the ultra-narrowband system under study.
- As the project title indicates, ultra-narrowband systems that do not exceed 1 kHz of bandwidth will be considered.
- As a special case, the Low Earth Orbit (LEO) satellite channel will be studied, understanding LEO satellites as those satellites that have an altitude from the surface of the Earth of between 160 and 2000 km.
- In order to have an efficient code, the computational complexity of the simulator ought to be as low as possible.

Moreover, during the development of the project the following specifications have been taken into account.

- MatlabR has been the computing environment used in this project.
- The multiuser access mechanisms considered to access the network will be the four combinations of pure or slotted ALOHA in time or frequency domains.
- The main information sources for this project will be both information given by the project supervisor and information acquired by reviewing the literature, being the first option the dominant.

1.3 Time Planning

The realization of this project lasted five months. On the beginning of February 2017, the objectives of this work were being proposed and some research was performed in order to get in touch with the subject under study. During the rest of February and during March, P2P simulation was being

developed and the PHY aspects of the project were being performed. Later on, on the end of May, all the MAC aspects were already studied. The analysis and conclusions of the thesis were finished on mid-June.

		DURATION TIME [weeks]																	
		February				March				April				May				June	
		1 st	2 nd	3 rd	4 th	1 st	2 nd	3 rd	4 th	1 st	2 nd	3 rd	4 th	1 st	2 nd	3 rd	4 th	1 st	2 nd
WORK PACKAGE	1	X																	
	2	2.1					X												
		2.2							X										
	3	3.1											X						
		3.2													X				
4																			

Figure 1: Gantt Diagram of the Time Planning for this project.

A structure of the evolution of the developed work is shown the previous Gantt Diagram. The crosses represent the weeks in which meetings with the supervisor were held. The numbers of the work packages correspond to the following ones:

1. Preparation
2. PHY Aspects
 - (a) P2P
 - (b) PHY Aspects Analysis
3. MAC Aspects
 - (a) Standard ALOHA
 - (b) Satellite ALOHA
4. Analysis and Conclusions

1.4 State of the Art

IoT basically consists on the inter-networking of physical devices embedded with electronics, software, sensors and so on which enable these objects to collect and exchange data. This relatively new concept is gaining more and more interest throughout the years, because of its interesting promise to integrate connectivity solutions with sensors, actuators and meters.

The main challenge of this paradigm is to let a huge number of devices be connected at a low cost, with a limited infrastructure and featuring a very long-life time with mild energy requirements.

As stated in [1], two technologies are being researched at this moment. The first one relies on broadening the capabilities of cellular technologies especially with the preparation of the future 5G. Nevertheless, the challenges posed by IoT services make difficult their integration into the cellular networks, which are originally devised to support broadband communications. Usually, IoT devices have long range capabilities and transmit small packets with very few transmissions

per day. Based on that, the second strategy relies on the deployment of a new network technology which may better comply with the specific features of IoT, e.g. massive machine communications with burst transmissions. In this sense, it is desirable to reduce the overhead in the access procedure as much as possible, which calls for access schemes with a reduced signalling.

An interesting approach to IoT is the one offered by the 3rd Generation Partnership Project (3GPP), which addresses the case in which networks offer wide-area coverage, in which complexity reduction, long battery lifetime and backward compatibility are the main objectives. The concept of NB-IoT, shares these objectives and aims to offer a lean network design allowing operators to introduce IoT applications using a small portion of its existing available spectrum.

Nowadays, four different technologies dedicated to IoT are being investigated, namely, UNB, Chirp Spread Spectrum (CSS), Weightless and Random Phase Multiple Access (RPMA).

CSS transmission occupies a bandwidth much larger than what is actually needed for the considered data rate and takes advantage of the controlled frequency diversity to recover data from weak signals. On the other hand, Weightless-N (the first version of Weightless) implements NB technology using DBPSK and frequency hopping algorithm in order to counteract interference and fading. RPMA is based on Direct Sequence Spread Spectrum (DSSS) and also uses DBPSK modulations, before being spread by a Gold Code. Finally, the signal is randomly delayed before transmission.

This project focuses on the use of UNB systems as they have been shown to be a suitable option for long distance transmissions, exhibit robustness against the interferences and keep low the energy consumption, which are the three key ingredients of major importance in the IoT context.

2 PHY Layer: Point to Point Communications System

2.1 Introduction

The scope of this chapter is to describe an UNB P2P communication system, giving special emphasis to the physical layer aspects.

In section **2.2**, a simple point to point baseband communication system is developed. Later on, this simulation is extended to a passband system and its characteristics are studied. In section **2.3**, the previous simulation is extended to analyse a differential modulation (in this project the modulation used has been DBPSK) and its robustness to the phase offset induced by the channel. Different shaping pulses are analysed in section **2.4** and its main characteristics are compared. Finally, in section **2.5**, a chapter overview and some conclusions are stated.

2.2 P2P

In order to be able to study the behavior of different aspects of the PHY of UNB systems, a simple point to point communication system is simulated in a MATLAB environment.

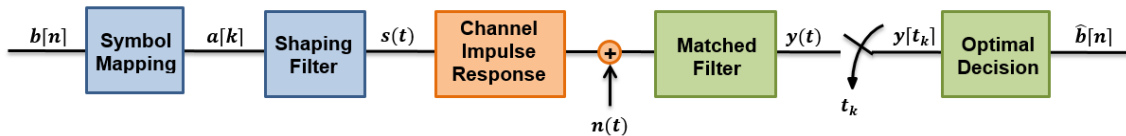


Figure 2: Scheme of a baseband communications system.

The first system follows the classic baseband communication scheme shown in *Figure 2*. A sequence of random binary digits $b[n]$ are generated and are encoded with a Binary Phase-Shift Keying (BPSK) modulation becoming $a[k]$. This signal goes through the shaping filter where the symbols are convoluted with a Square-Root Raised Cosine (SRRC) pulse with a roll-off value of 0.5. This signal, referred to as $s(t)$ is contaminated by Additive White Gaussian Noise (AWGN), the power of which is $N0$. At the receiver, the signal goes through the matching filter $h_{MF}(t)$, later on the symbols are recovered following the Maximum A Posteriori (MAP) criteria and finally bits are decoded.

The system model is described as follows:

$$s(t) = \sum_{n=-\infty}^{\infty} a[n]p(t - nT)$$

$$h_{MF}(t) = p^*(-t)$$

$$y(t) = [s(t) + n(t)] * h_{MF}(t)$$

Where T is the symbol period. In *Figure 3*, a realization of the transmitted and the received signal is depicted. As for the received signal, different noise values have been simulated, yielding a Signal-to-Noise Ratio (SNR) of 14dB and 50dB.

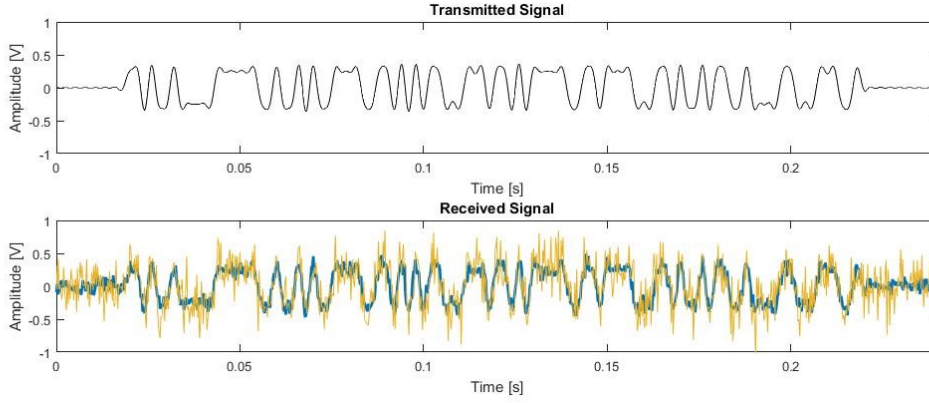


Figure 3: Transmitted signal and two received signals with different N_0 .

An important variation of this first communication system is its extension to a passband system. In almost all networks, signals are transmitted at a certain band, becoming passband communications.

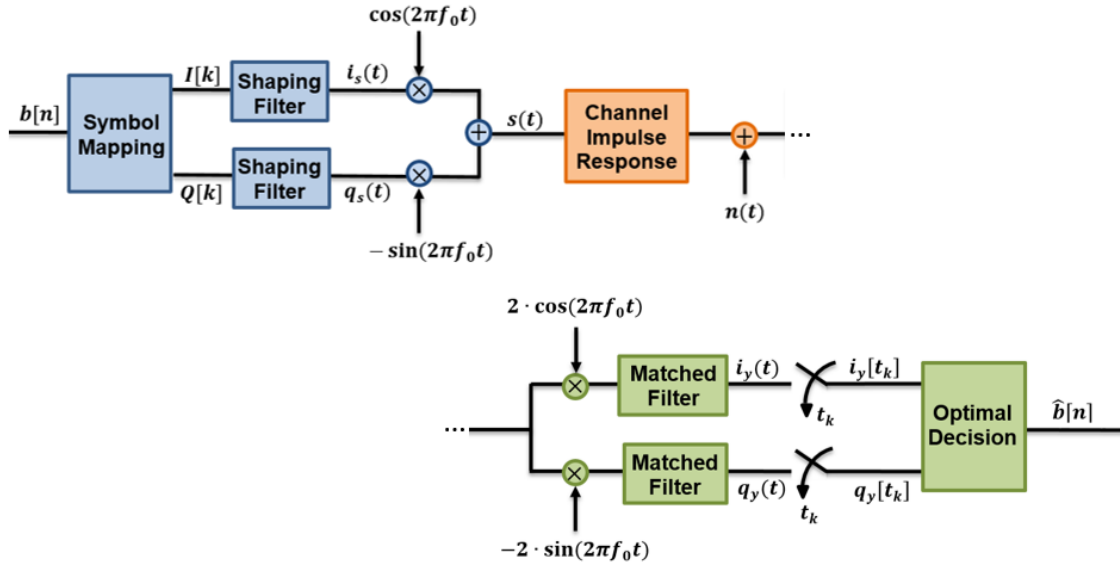


Figure 4: Scheme of a passband communications system.

The scheme of a passband communication is very similar to the baseband one. However, in order to move the band at which the system transmits, the signal must be modulated and later on demodulated. Moreover, in this simulation, the chosen modulation to work with is Quadrature Phase-Shift Keying (QPSK), which generates complex-valued symbols, changing a little bit the scheme.

The main equations followed by the baseband system using a QPSK modulation are:

$$B[k] = I[k] + jQ[k]$$

$$b_s(t) = \sum_{n=-\infty}^{\infty} B[n]p(t - nT)$$

$$s(t) = \Re[b_s(t)e^{j2\pi f_0 t}]$$

Where $B[k]$ is the transmitted symbol modulated with QPSK. The same analysis as the one developed in the baseband system with the same modulation is performed and it is verified that the BER curve is the same in both cases. On the other hand, by using the Welch estimator, it is checked that the Power Spectral Density is centered at different frequencies, as it is shown in *Figure 5*.

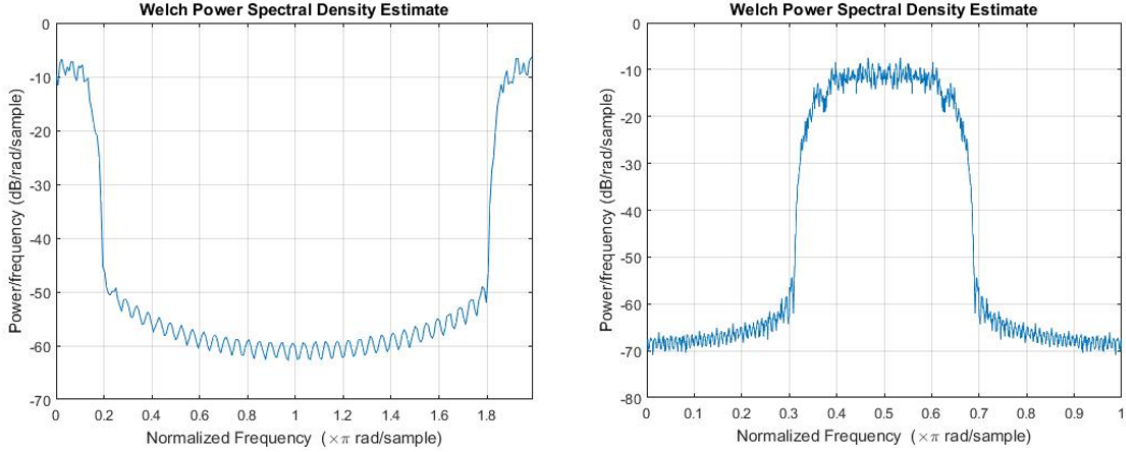


Figure 5: Power Spectral Density Estimation of the baseband signal and of the passband signal.

2.3 Differential Modulations

Differential modulations such as DBPSK are excellent candidate solutions to the problem of the phase offset introduced by the channel, for their input information is included on the phase difference of two successive signaling elements, not in its absolute phase. This kind of modulations are frequently used in wireless communications systems. Therefore, for this project the differential modulation chosen in order to study its robustness against the phase offset is the DBPSK, the ideal encoder and decoder of which are shown in *Figure 6*.

- **Encoder:** $\bar{d}_k = b_k \oplus d_{k-1}$
- **Decoder:** $b_k = \bar{d}_k \oplus d_{k-1}$

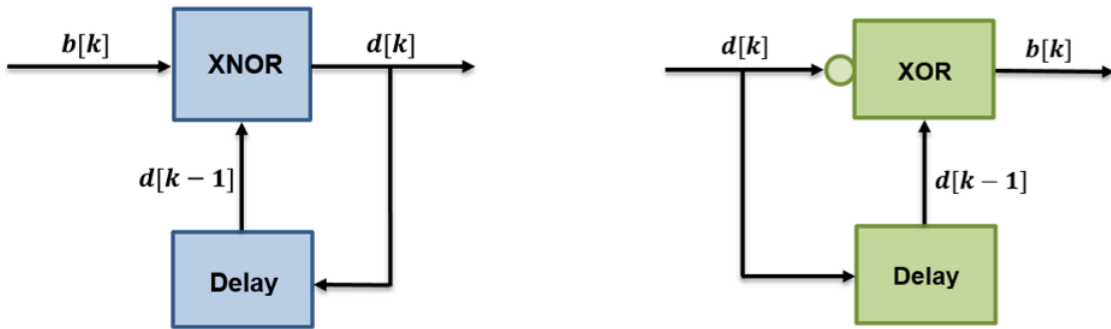


Figure 6: Scheme of the ideal DBPSK encoder and decoder.

The basic principle of a DBPSK modulation is not very complicated. The information bit that arrives at the input are XNOR operated with the previous bit. However, that would be the ideal case. In this project, a different approach has been used at the receiver, as it will be further explained. As the first bit has no other bit to be compared to, a reference bit is needed. The demodulator is no other thing than the inverse of the modulator. An example of a random binary input and its correspondent DBPSK output can be appreciated in *Figure 7*.

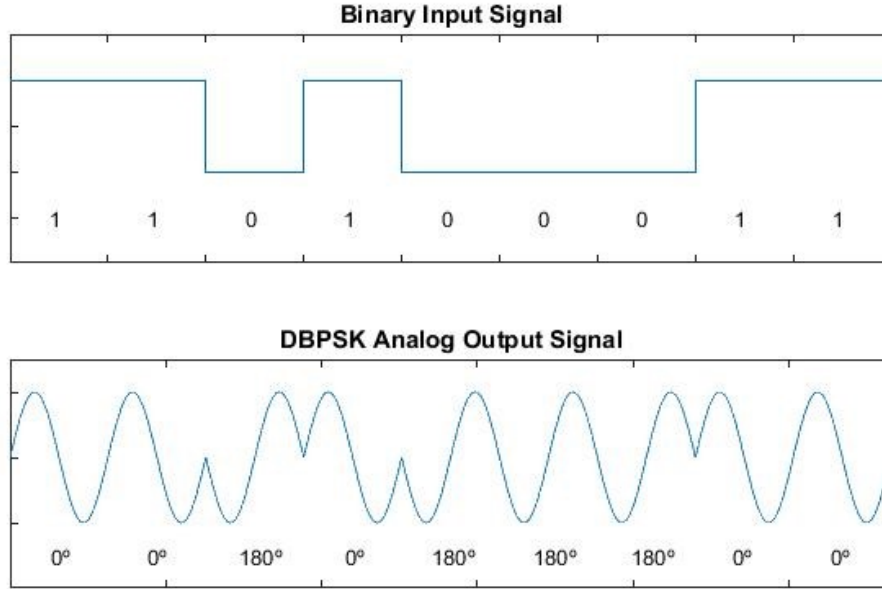


Figure 7: Example of a binary input with its correspondent DBPSK output.

To characterize the environment we worked with, according to the offset induced by the channel, the passband signal of a binary modulation was defined in the following way, where φ is a random number uniformly distributed between 0 and 2π .

$$s(t) = b_s(t)\cos(j2\pi f_0 t + \varphi)$$

Consequently, the received signal follows the equation:

$$r(t) = \sum_{n=-\infty}^{\infty} B[n]p(t - nT)\cos(j2\pi f_0 t + \varphi) + w(t)$$

Although BPSK is a real modulation, phase and quadrature are recovered in order to counteract the phase offset introduced by the channel. Consequently, at the input of the demapper de signal is given by:

$$y[n] = B[n]e^{j\varphi} + w[n]$$

where $w[n]$ is the filtered noise. It has been assumed that the pulse satisfies the Nyquist constraint.

The offset value is not known at the receiver but, as DBPSK is a differential modulation, this value is eliminated from the bit sequence when a received bit is multiplied for the conjugated version of its previous bit, as it can be seen in the following equation:

$$\Re(y[n]y[n-1]^*) = B[n]B[n-1] + w[n]B[n-1] + B[n]w[n-1]^* + w[n]w[n-1]^*$$

This way the bit sequence is recovered as if there was no phase offset although the noise is enhanced. However, as the phase of the first bit cannot be estimated for it has no reference, an additional bit has to be transmitted. In this project, a sequence of longitude N+1 has been transmitted and it has only been computed the BER of the N last bits, ignoring the first one.

For each iteration developed in this part of the project, the BER of the system is computed acquiring this way the typical BER in function of the SNR curve, which will be shown when comparing different modulations. In order to achieve reliable values, an order of thousands of trials are developed for each N_0 value.

In Figure 8, it can be appreciated that the fact of having a phase offset does not affect the BER of the DBPSK modulation. Moreover, the comparison between DBPSK, QPSK and BPSK can be acknowledged.

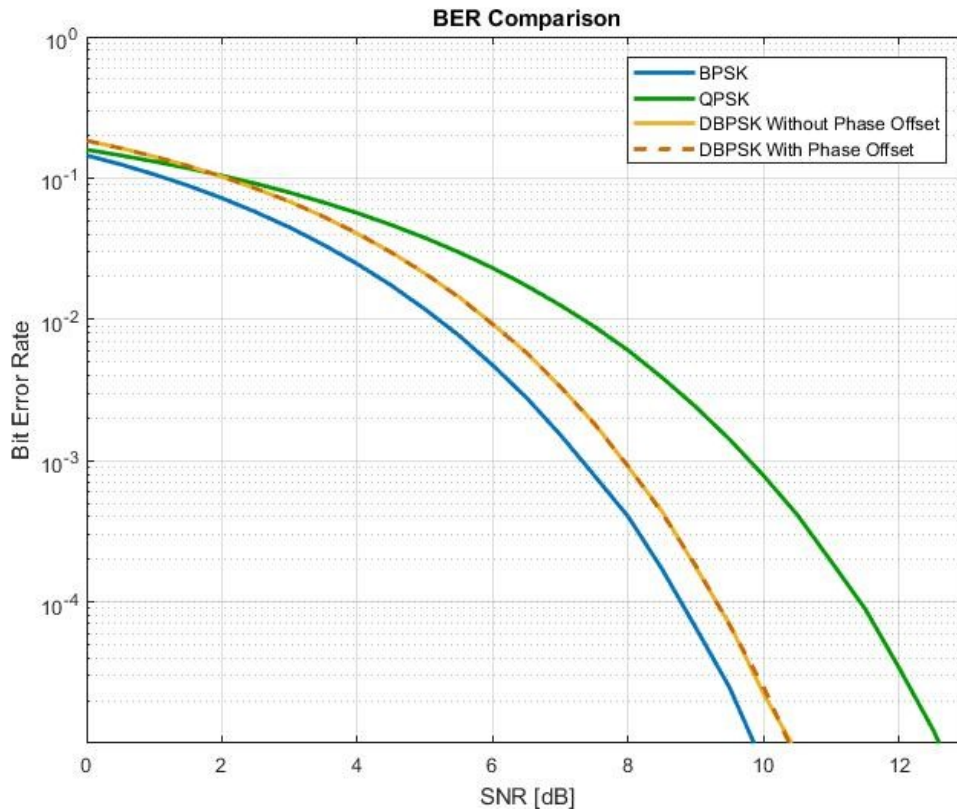


Figure 8: BER comparison using different modulations and a SRRC pulse.

One may note that the Differential version of a BPSK has a worse error rate than its classic version. However, given its perfect response to phase offsets, its BER deterioration is not that relevant. Furthermore, it still has a better error rate than a QPSK.

2.4 Shaping Pulses

The shaping pulses used in the point to point communications system are an interesting topic to analyze. In this project three shaping pulses will be analyzed: SRRC and two digital phase modulations constructed by the superposition of Amplitude Modulated Pulses (AMP) used as filters, which are used in GMSK.

Until this point, the SRRC has been used. This SRRC is one of the most common shaping filters used in digital communications and it is basically an implementation of the Nyquist filter, which exhibits an odd symmetry of about $1/2T_s$, where T_s is the symbol-period of the communication system. This filter is also characterized by its roll-off factor β , which is a measure of the excess

bandwidth. The typical temporal impulse response of a SRRC filter is the following one:

$$h(t) = \begin{cases} \frac{1}{T_s} \left(1 + \beta \left(\frac{4}{\pi} - 1\right)\right), & t = 0 \\ \frac{\beta}{T_s \sqrt{2}} \left[\left(1 + \frac{2}{\pi}\right) \sin\left(\frac{\pi}{4\beta}\right) + \left(1 - \frac{2}{\pi}\right) \cos\left(\frac{\pi}{4\beta}\right) \right], & t = \pm \frac{T_s}{4\beta} \\ \frac{1}{T_s} \frac{\sin\left[\pi \frac{t}{T_s} (1 - \beta)\right] + 4\beta \frac{t}{T_s} \cos\left[\pi \frac{t}{T_s} (1 + \beta)\right]}{\pi \frac{t}{T_s} \left[1 - \left(4\beta \frac{t}{T_s}\right)^2\right]}, & \text{otherwise} \end{cases},$$

In the shaping pulse comparison part of this project, the value of the roll-off factor has been 0.5, however, in the following picture, a behavior of a SRRC pulse with different roll-off factors can be appreciated.

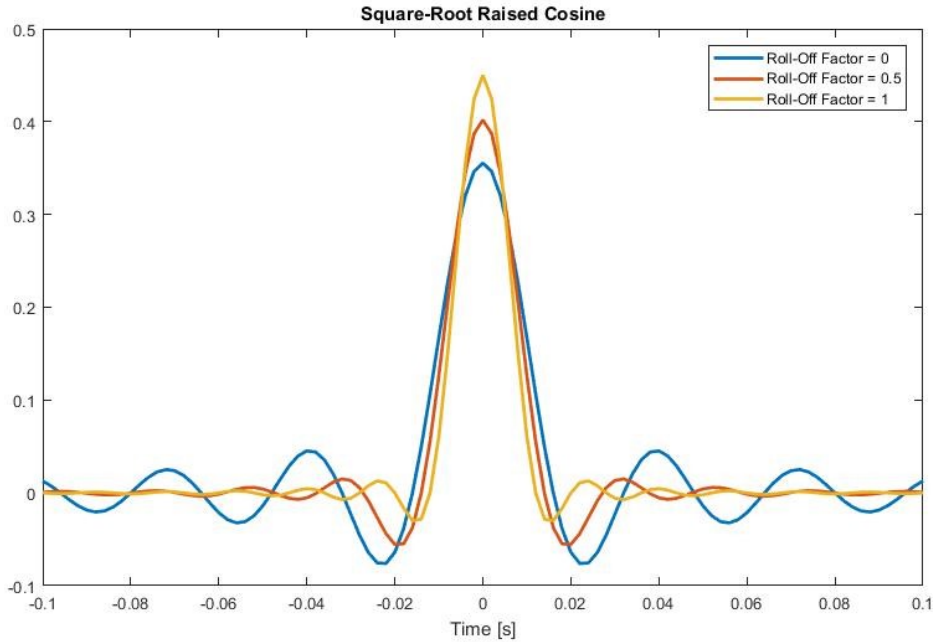


Figure 9: Square-Root Raised Cosine temporal representation for different roll-off factor values.

The next two pulses under study are those coming from digital phase modulations constructed by the superposition of AMP. These two pulses are used in the linear model of Minimum Shift Keying (MSK) and the GMSK.

It has been shown in [3] that any constant amplitude binary phase modulation can be expressed as a sum of a finite number of time-limited amplitude modulated pulses. This procedure, also known as AMP decomposition, has advantages both from a theoretical point of view (computation of autocorrelation and frequency spectrum) and from a practical one (design of modulators and demodulators).

The creation of this procedure is deeply detailed in [3] and will not be explained because it is beyond the scope of this project. Furthermore, the simulation code needed for this study was already given at the beginning of the semester.

It is worth mentioning that MSK and GMSK modulations, actually implement a DBPSK. GMSK is very similar to the standard MSK however, the data stream is shaped with a Gaussian filter. When using a simple MSK modulation, the resulting equation for the transmitted signal is the following one, where θ_0 is a constant phase which will be ignored hereafter.

$$s(t) = e^{j[\theta_0 + \sum_{n=-\infty}^{\infty} B[n]\varphi(t-nT)]}$$

After several derivation steps shown in [3] the signal is simplified and the pulse is transformed from $\varphi(t)$ into $p(t)$. The resulting signal can be expressed as:

$$b_s(t) = \sum_{n=-\infty}^{\infty} j^n B[n]p(t-nT)$$

$$s(t) = \Re[b_s(t)e^{j2\pi f_0 t}]$$

In this project, the MSK pulse that will be under study is a pulse that spans one symbol period, i.e. $L=1$, which is shown in *Figure 10*.

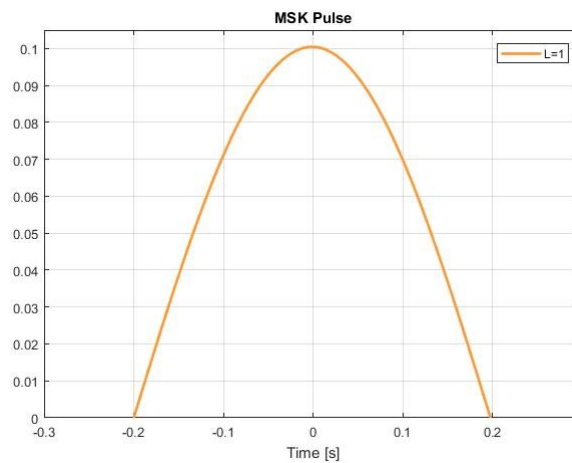


Figure 10: Representation of a MSK Pulse of Length = 1.

The final two pulses that will be analyzed on this project are the GMSK with lengths $L=1$ and $L=4$, in terms of symbol periods. The representation in the temporal domain of those pulses is shown in the following graphic.

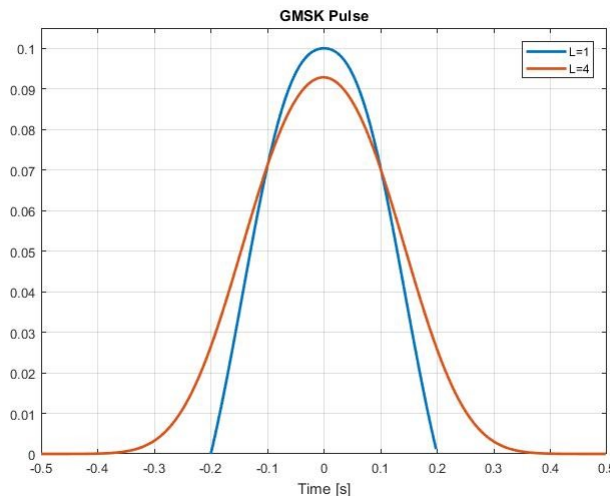


Figure 11: Representation of GMSK Pulses of Length = 1 and Length = 4.

As mentioned before, in this project, the three different pulses presented are evaluated with different lengths. Three characteristics of these pulses are chosen to compare them, which are the BER, the PSD and its PAPR.

To evaluate the BER obtained by the use of these pulses, the last simulated environment (DBPSK P2P communication system) is explored. Five different simulations are performed using in each one a different shaping pulse with different lengths and their error rates can be appreciated in *Figure 9*. From that figure, it can be stated that the error rates are almost the same, so the BER cannot be taken as a parameter when evaluating the performance of these different pulses. However, it can be appreciated that the SRRC pulse that has a length of $L=1$ in terms of symbol period, has the worst BER.

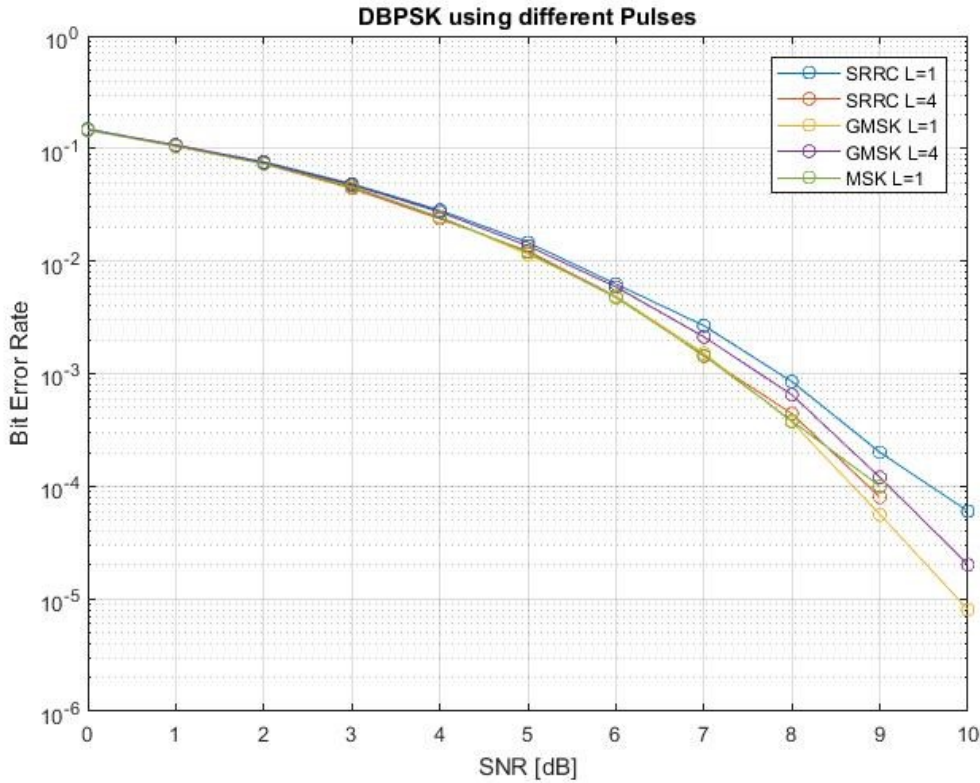


Figure 12: BER comparison using different shaping pulses.

The next characteristic to be evaluated is the PSD of each pulse, which is given by $p(t)$. Once the pulses are created, their PSD is computed as the square of the absolute of its Fourier Transform. The following formula gives the PSD of a pulse in a logarithmic scale.

$$S_{PP}(f) = 20 \log_{10}(|FT[p(t)]|)$$

To guarantee a correct performance of the communication system, it is very important that the PSDs of the shaping pulses show a large Side Lobe Level (SLL), in order to avoid interferences to adjacent channels.

In *Figure 13* the PSDs of each pulse are shown. It can be clearly seen that the pulses that show a best behavior in terms of best PSD are the SRRC pulse of $L=4$ and the GMSK pulse also with a $L=4$.

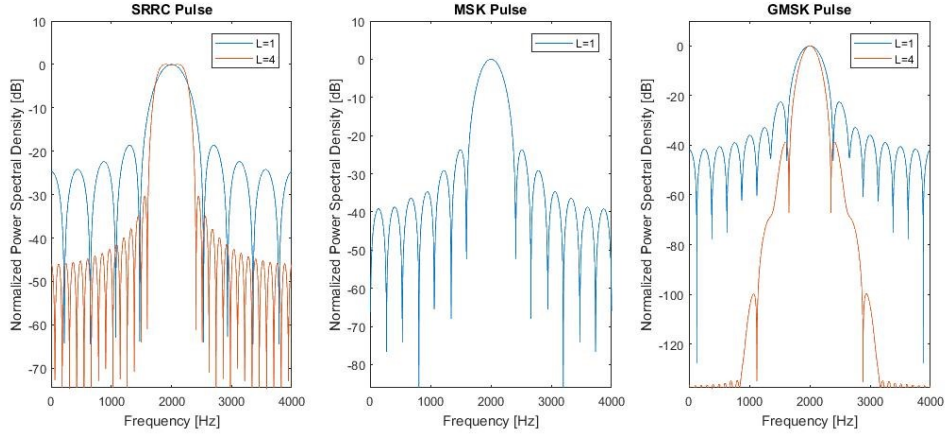


Figure 13: PSD comparison using different shaping pulses.

The next parameter used to evaluate different pulse behavior is the PAPR, which is often used to characterize digitally modulated signals. It is the peak amplitude squared divided by the Root Mean Square (RMS) value squared.

$$PAPR[dB] = 10 \log_{10} \frac{|b_s(t)|_{peak}^2}{b_s(t)_{rms}^2}$$

Nonetheless, as the PAPR for a random signal is a statistical quantity, the probability of a given peak power must be found. Therefore, the PAPR is normally represented as a function of the Complementary Cumulative Distribution Function (CCDF) for a given frame length. This function, for a given distribution function X , evaluated at x , gives the probability that X will take a value higher to x . The equation of this concept is the following one.

$$CCDF(x) = P(X > x)$$

In the case of this project, the function being evaluated is not a random variable x , it is the PAPR. Therefore, the computed CCDF that will be the same but evaluating the Peak to Average Power Ratio as explained before.

$$CCDF(x) = P(PAPR > x)$$

Obviously, it is desired to have low PAPR values, for the CCDF function should steeply decrease at the lowest values of x possible.

The PAPR and CCDF computation was developed for all five pulses under study as it can be appreciated in *Figure 14*. This graphic was done given the values found in a MATLAB simulation in which the PAPR values were computed as indicated in the PAPR formula, later on its CCDF function was found from a closed loop that used the CCDF formula definition.

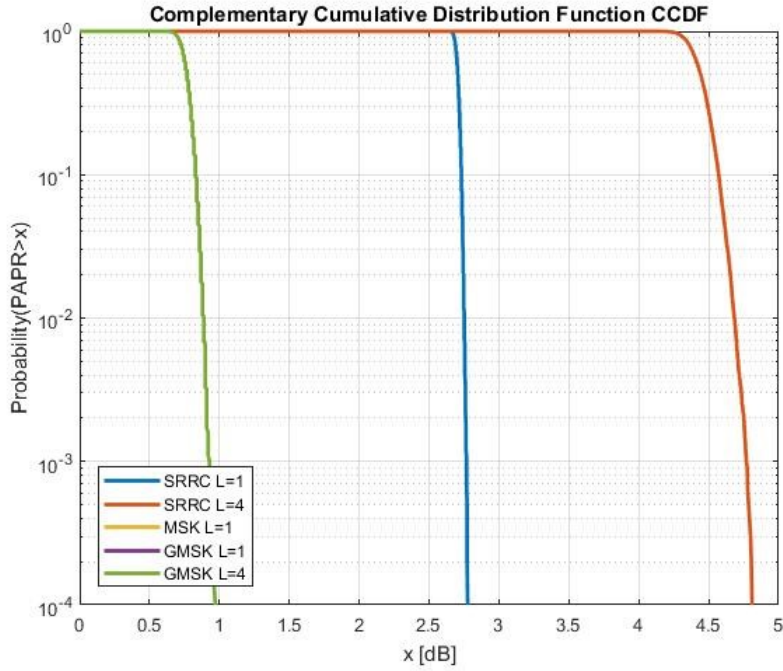


Figure 14: CCDF comparison using different shaping pulses.

In *Figure 14*, the CCDF functions from the pulses can be appreciated. However, values from the MSK pulse and the GMSK pulse with $L=1$ are so close to 0 dB that cannot be appreciated. Therefore, it can be said that these two pulses are the best options in terms of PAPR analysis, for the probability for their PAPR values to be high are very low.

2.5 Conclusions

In this section, two main conclusions can be drawn. First of all, it has been shown in *Figure 8* that differential BPSK modulation is an excellent option for a UNB communication both for its robustness to phase variations and its acceptable error rate.

Furthermore, a shaping pulse analysis has been developed. As it has been shown in *Figure 12*, all five pulses present a very similar BER, for that characteristic is not relevant when determining which pulse is better for a UNB communication system.

Nevertheless, relevant information can be taken from the study of the PSD of each pulse. As it has been said before, the pulses that show a best behavior in terms of best PSD are the SRRC pulse of $L=4$ and the GMSK pulse also with a $L=4$.

Moreover, from the PAPR analysis developed before, it is concluded that the two best shaping pulses concerning the PAPR characteristic are both the MSK pulse and the GMSK pulse with $L=1$.

Pulse	L_p	BER	PSD	PAPR
SRRC	1	-	③	③
	4	-	❶	④
MSK	1	-	②	❶
GMSK	1	-	④	❶
	4	-	❶	②

All these characteristics are summarized in the previous table, from where it can be concluded that the best options in an UNB system are both the MSK pulse with $L=1$ (although its PSD characteristic is not the best, its PAPR behavior is excellent), and the GMSK pulse with $L=4$. Therefore, the choice of the shaping pulse in a UNB system should be between these two pulses, choosing between them depending whether if the strongest requirement is the PSD or the PAPR.

3 MAC Layer: Random Access Schemes

3.1 Introduction

In the previous chapter, the physical aspects of an UNB communications system have been analysed. However, in this chapter the work is focused on the MAC layer of the system, in other words, the random-access schemes typical from an UNB communication system are studied. In section **3.2**, four different types of ALOHA access schemes are simulated and its main characteristics such as the throughput and the collision probability are thoroughly studied. Later on, in section **3.3**, the access scheme is extended into a satellite system in which the Doppler effect has an impact on the performance, which are analysed. Finally, in section **3.4**, a chapter overview and some conclusions are stated.

3.2 ALOHA Schemes

Low cost oscillators for the carrier generation are used in order to have a limited node cost. In UNB systems the lack of precision of these oscillators is irrelevant. If the jitter of the oscillator is significantly lower than the signal bandwidth (lower than 1kHz), the performance is not degraded.

However, with uncertainties higher than the signal bandwidth it is impossible to obtain non-overlapping frequency channels with reasonable frequency guard bands. This leads to discard classical transmission schemes based on frequency channelization and focus on other multiple access schemes, such as the ALOHA protocol. In particular, it has been proved that the lack of precision from which UNB signals suffer, makes them behave similarly to a frequency unslotted random access.

In this project, the four following random time-frequency access schemes have been studied:

- **FUTU:** Frequency Unslotted Time Unslotted
- **FUTS:** Frequency Unslotted Time Slotted
- **FSTU:** Frequency Slotted Time Unslotted
- **FSTS:** Frequency Slotted Time Slotted

The unslotted ALOHA protocol is based on a random-access technique with the following procedure. A set of devices are connected to a base station. Once a device has data to send, it begins to transmit following no kind of restriction, at the frequency and time it wants to transmit.

Meanwhile, in the slotted version of this protocol, when a device wants to transmit, it waits for a temporal slot to begin and then it begins to transmit in a given subchannel. FUTS and FSTU versions are just hybrids of these two types of ALOHAs.

Regarding the reception part, if the system receives more than one packet at the time and frequency position, then all packets are dismissed. *Figure 15* tries to exemplify the behavior of the four ALOHA schemes under study.

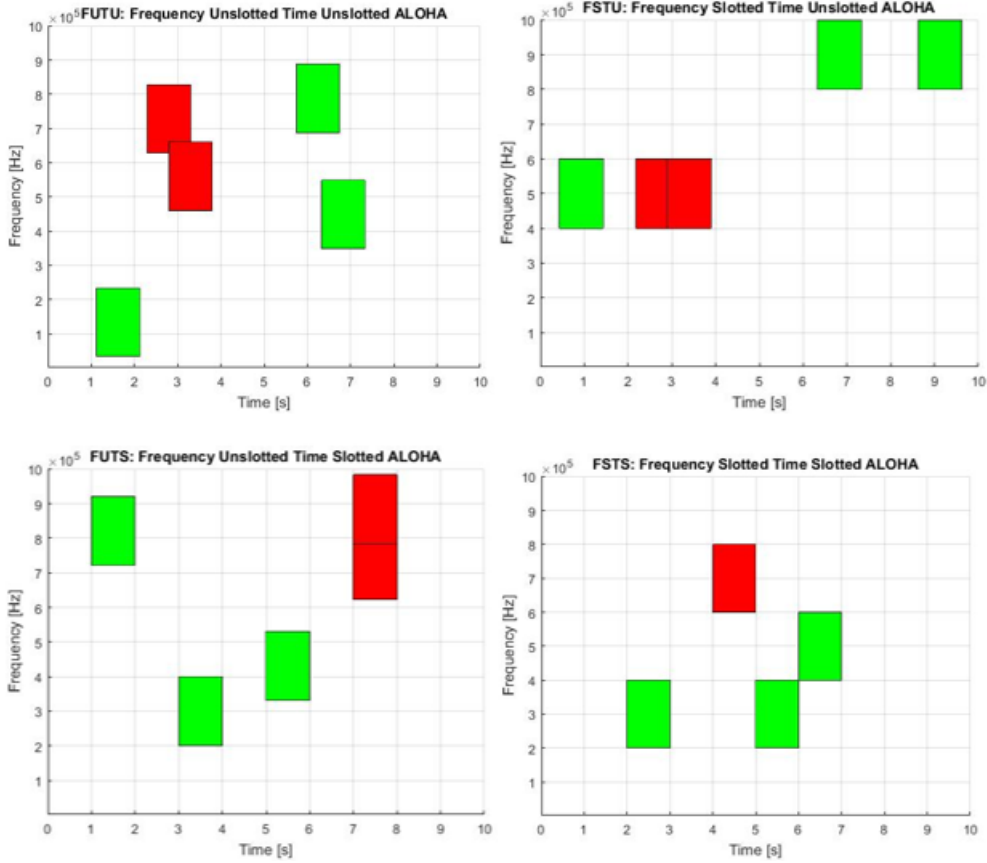


Figure 15: Distribution examples of different ALOHA schemes.

Four simulations, one for each ALOHA scheme, are run with a transmission time per packet (or temporal slot) of $\tau = 0.5s$, a total time window of $T = 10s$, a packet bandwidth (or frequential slot) of $b = 500Hz$ and a frequency window of $B = 200kHz$.

A relevant issue not taken into account in the developed simulations was the tail effect, which happens in the time domain. To exemplify this issue, this effect in the time domain will be detailed. In this case, a total time window of $T = 10s$ is chosen to analyze the characteristics of the protocols. In this window, packets randomly appear and collisions occur depending the number of active users. Only the packets in the time window of interest are taken into account when determining the throughput, the collision and detection probabilities. However, packets that appear in the previous or following windows are not considered, so that some collisions at the edge of the window are not accounted for. However, if the duration of the window is sufficiently higher than the packet duration, then it can be assumed that the tail effect is negligible.

Notwithstanding, as the total window values chosen for all cases are larger than packet transmission times, the tail effect is barely noticed in the results. However, it is the cause of the minimum deviations from which the figure's curves suffer.

In order to be able to analyze the features of the four ALOHA schemes under study, the main characteristics of these schemes are straightforward studied but firstly, few parameters must be defined. The most common characteristic of an ALOHA is its throughput vs. load curve. The load G of the simulation is defined as follows:

$$G = n_{tran} \frac{\tau}{T} \frac{b}{B}$$

where n_{tran} is the total number of transmissions.

The throughput S of a system can be computed both for a theoretical case and for the practical one. In this thesis, theoretical and experimental throughput results will be compared. Concerning the closed-form expression of the throughput, it depends on α_t , which equals 1 for the time-slotted ALOHA and 2 for the time-unslotted version, and α_f , which equals 1 for the frequency-slotted ALOHA and 2 for the unslotted version.

The theoretical throughput has been defined following its theoretical formula, while the practical throughput has been defined as the number of successful transmissions multiplied for the portion of transmission time with respect to the total time window and the packet bandwidth with respect to the total system bandwidth.

$$S_{Theoretical} = Ge^{-\alpha_t\alpha_f G}$$

$$S_{Practical} = n_{suc} \frac{\tau}{T} \frac{b}{B}$$

where n_{suc} is the number of successful transmissions.

In *Figure 16*, the comparison between the theoretical curve and the practical one can be appreciated for each scheme. It can be seen that both curves are very similar for all configurations. The tiny deviation that occur might be due to the tail effect.

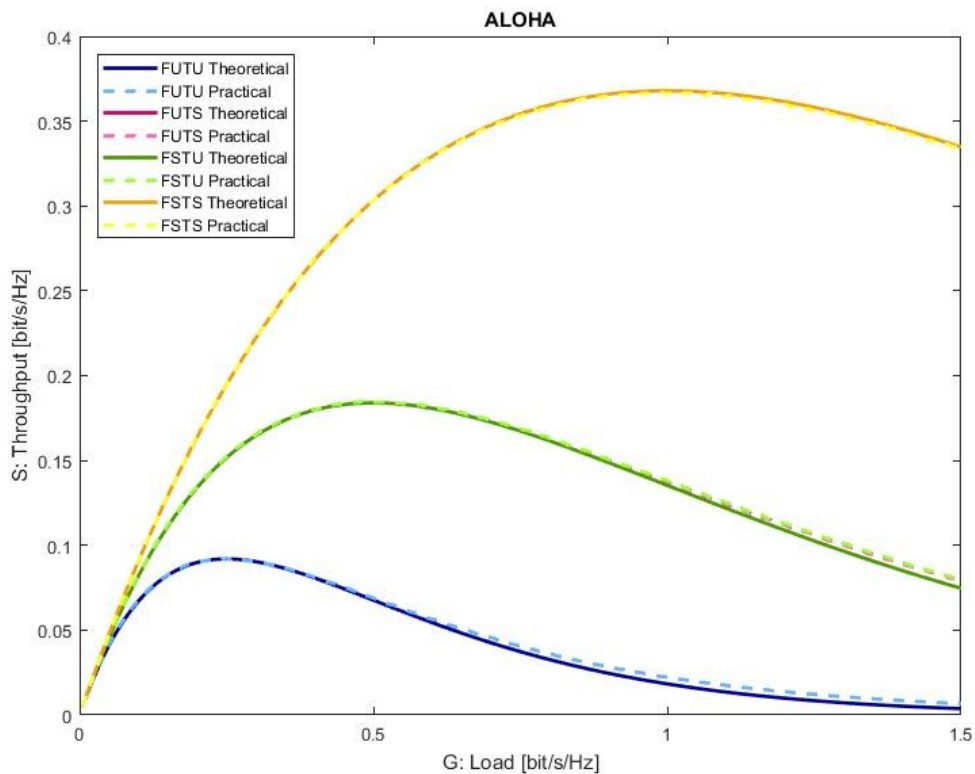


Figure 16: Throughput comparison of different ALOHA schemes.

As it can also be seen in the previous figure, the hybrid cases are if not the same, very similar. There is a relevant corollary explained in [4] that presents that time and frequency domain are dual in the ALOHA protocol. This means that time and frequency parameters can be indifferently interchanged in all the equations used for evaluation, because b/B equals τ/T . Other interesting characteristics to infer from ALOHA protocols are the collision and detection probabilities. The practical and theoretical collision probabilities are defined as the following equations show, where

G is the load and α_t and α_f are the same parameters as the ones defined before. For the practical case, the collision probability is defined as the number of collisions divided by the number of transmissions and averaged for several realizations.

$$P_{Theoretical}(col) = 1 - e^{-\alpha_t \alpha_f G}$$

$$P_{Practical}(col) = \frac{n_{col}}{n_{tran}}$$

where n_{col} is the number of collisions occurred.

In *Figure 17*, it can be appreciated that, for each scheme, the theoretical and the practical probabilities are exactly the same.

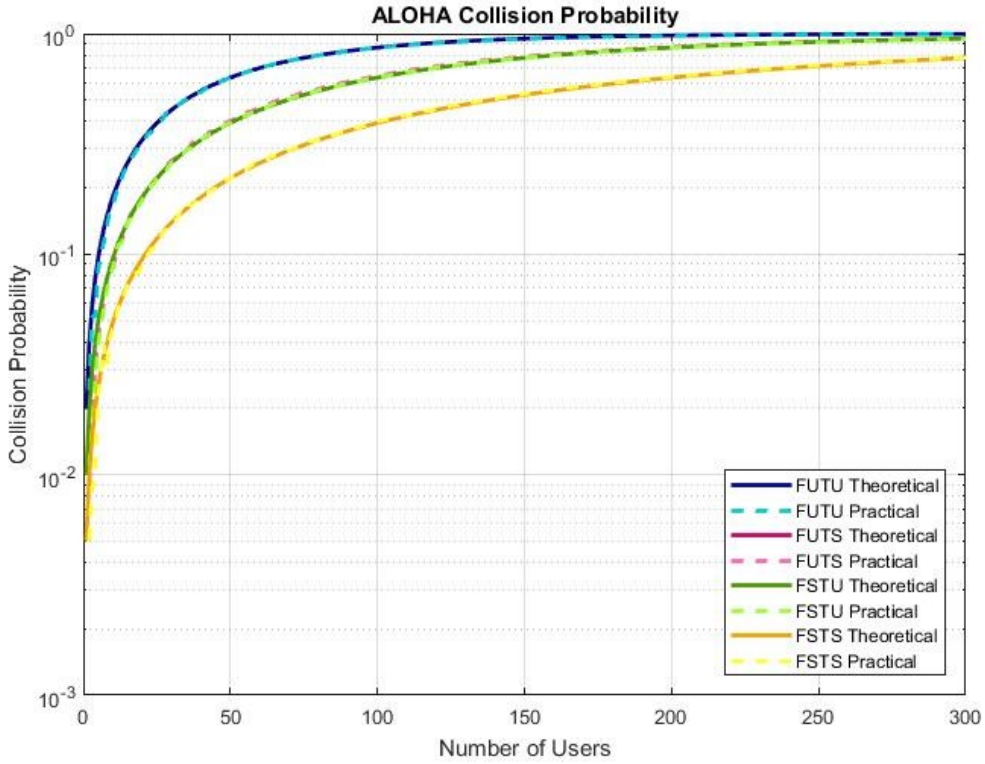


Figure 17: Collision probability comparison of different ALOHA schemes.

The practical and theoretical detection probabilities are defined as the following equations show. The detection probability is the complementary to the collision probability.

$$P_{Theoretical}(det) = e^{-\alpha_t \alpha_f G}$$

$$P_{Practical}(det) = \frac{n_{suc}}{n_{tran}}$$

In *Figure 18*, it can be appreciated that, for each scheme, the theoretical and the practical probabilities are exactly the same. For example, from that figure it can be stated that the probability of a packet being detected in a FUTU ALOHA scheme with 5 users is exactly of 0.9.

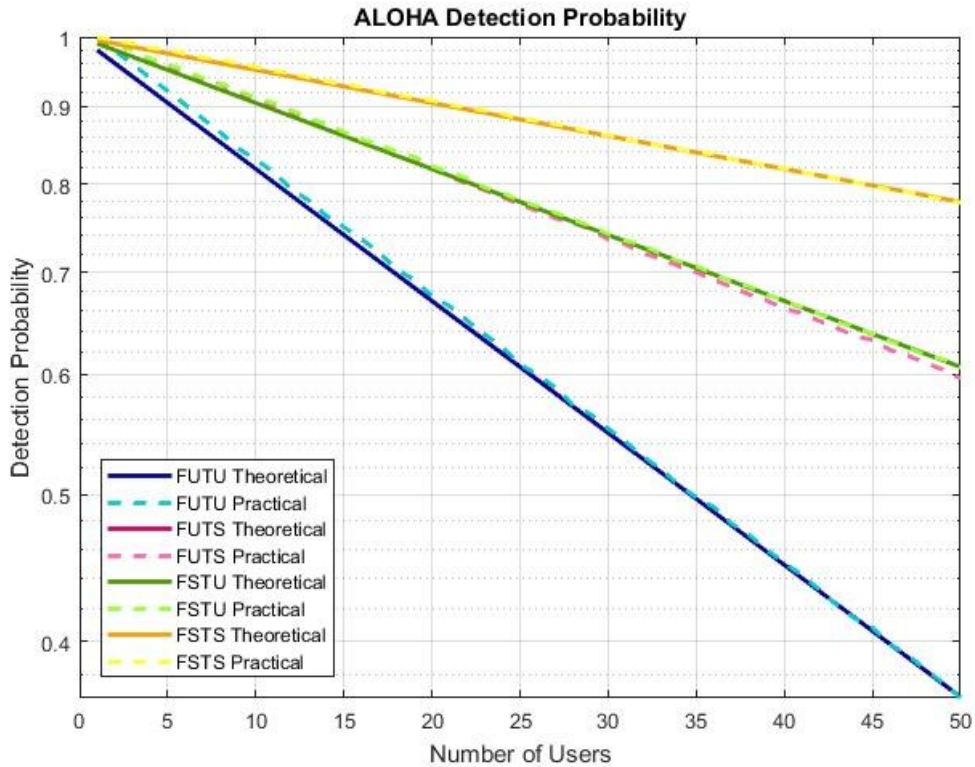


Figure 18: Detection probability comparison of different ALOHA schemes.

From the three previous figures, some relevant conclusions can be drawn. It can be clearly seen that the FSTS is the best scheme, for the time frequency space is divided into orthogonal channels, minimizing the probability of collision. Moreover, the FUTU scenario is the worst one, as partial overlapping is possible both in time and frequency domain.

However, as in practice both precise frequency and timing are difficult to be achieved simultaneously, because require an accuracy that cannot be easily attained. In addition, the signalling is substantially increase, yielding an overhead that reduces the energy efficiency. Thanks to the previously explained duality that exists between time and frequency with the selected parameters, the resultant curves from the hybrid cases is the same in all three figures. FSTU and FUTS seem to be the best options because improve the performance with respect to the pure ALOHA and relax wither time or frequency constraints, depending on the characteristics of the devices and the system. Moreover, although the FUTU scheme shows the worst behaviour in the previous figures, it is still an option due to its implementation simplicity for it requires no kind of signalling which makes it cheaper and more efficient.

3.3 Satellite Access

The use of satellite communications is endorsed by the possibility of providing Internet access to rural, remote and maritime environments, where there is no terrestrial infrastructure.

However, among all the impairments that satellite communications must face, a concrete one will be straightaway under study. This relevant impairment is the Doppler shift in Non-Geostationary Satellite Orbits (NGSO), which is a frequency deviation that appears when the satellite is moving at a certain velocity with respect to the earth terminal. This effect depends on the operating frequency, the angular velocity of the satellite, and its orbital position, as it is shown

in [5].

$$f_d(t) = \frac{f_0 \omega_{sat} R_E \cos(\vartheta(t))}{c}$$

The orbital position of the satellite is evaluated in the Doppler shift formula by its Nadir angle, which is related to the elevation of the ground station with respect to the satellite as it is hereby shown.

$$\vartheta(t) = \sin^{-1} \frac{R_E \cos(El)}{R_E + h}$$

To be able to correctly analyze the impact of the Doppler effect on the MAC layer of a communication system it is important to study different scenarios in which the elevation varies. The change in the elevation value is due to many possibilities. The following scheme illustrates one of these possibilities, in which the same station is connecting to an orbiting satellite.

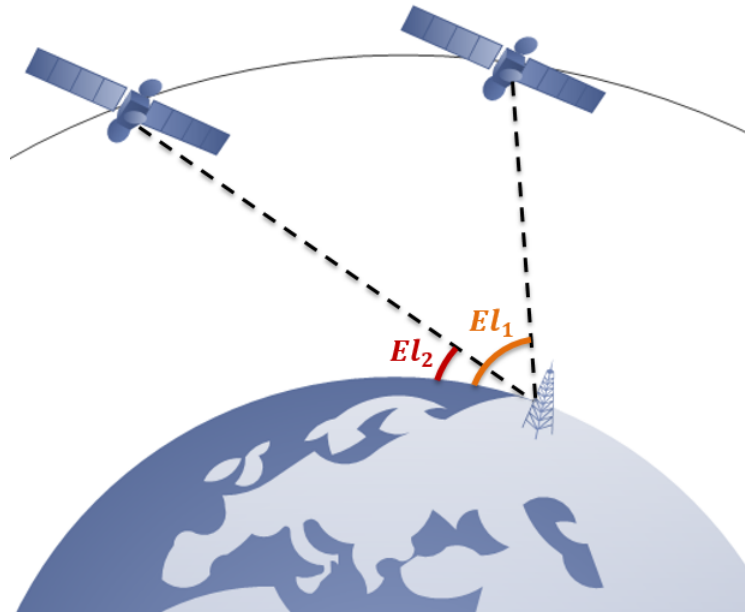


Figure 19: Example of different elevation values in a satellite environment.

It also happens that different users try to access the same satellite from different positions, having this way different elevation angles. Therefore, in this project, it is important to study all different cases in which the elevation varies. For this study, it has been assumed that connectivity can only be achieved if the elevation angles are between 45° and 135° .

Taking advantage of the simulations developed in the previous section to analyze the MAC characteristics of a communication system, a new simulation environment is created in which the Doppler effect is taken into account. When the satellite is visible, the position of the user is random, which means that the elevation angle could take any value between 45° and 135° . This Doppler shift is added to the randomly selected frequency in which the packet will burst. Some of them therefore, exceed the original system bandwidth, but in this project, it is presumed that the adjacent frequential bands are not occupied and that the receiver is able to extend the sensed bandwidth to not lose the packets that are received out of the transmission band.

Therefore, most of the users' packets transmit the original bandwidth (blue area in the figure) but some of them intrude the new area, caused by the Doppler effect (white area). An example of a distribution of this kind of system is illustrated in *Figure 20*.

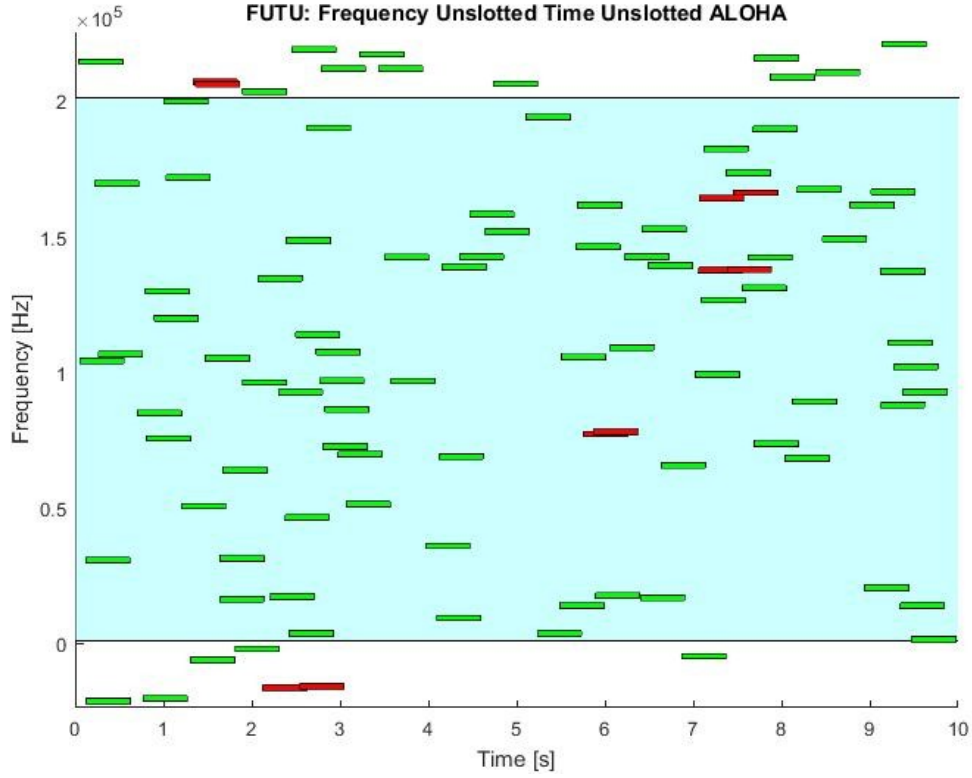


Figure 20: Distribution example of an unslotted ALOHA in a NGSO environment.

To be able to evaluate the behavior of this new system, a relevant simulation is performed using the following system parameters, most of them taken from [6] and typical from a LEO satellite.

- Satellite Orbit $h = 700km$ (LEO)
- Carrier Frequency $f_0 = 1.6GHz$
- Satellite Angular Velocity $\omega_{sat} = 0.727rad/s$
- Packet Transmission Time (or Temporal Slot) $\tau = 0.5s$
- Time Window $T = 10s$
- Packet Transmission Bandwidth (or Frequential Slot) $b = 500Hz$
- Frequency Window $B = 200kHz$
- Maximum Number of Users = 4000

The characteristics that will be analyzed of this new scheme are the collision and the detection probability. There is no point in analyzing the throughput as a function of the load because, as this new system also follows the ALOHA protocol, the curve was the same for the terrestrial and the satellite cases. Furthermore, no theoretical study has been developed in this case for the simulations' behavior has previously shown to be identical.

The case referred as terrestrial is a case in which the simulations from the previous study have been used, which means a static receiver. On the contrary, the one referred as satellite obviously refers to this new simulation in which the Doppler effect is taken into account. In both cases,

the unslotted ALOHA is the one implemented. If the Doppler is not compensated, which seems unrealistic for IoT devices, then unslotted ALOHA cannot be implemented. Collision and detection probabilities have been defined exactly the same way as in the previous section.

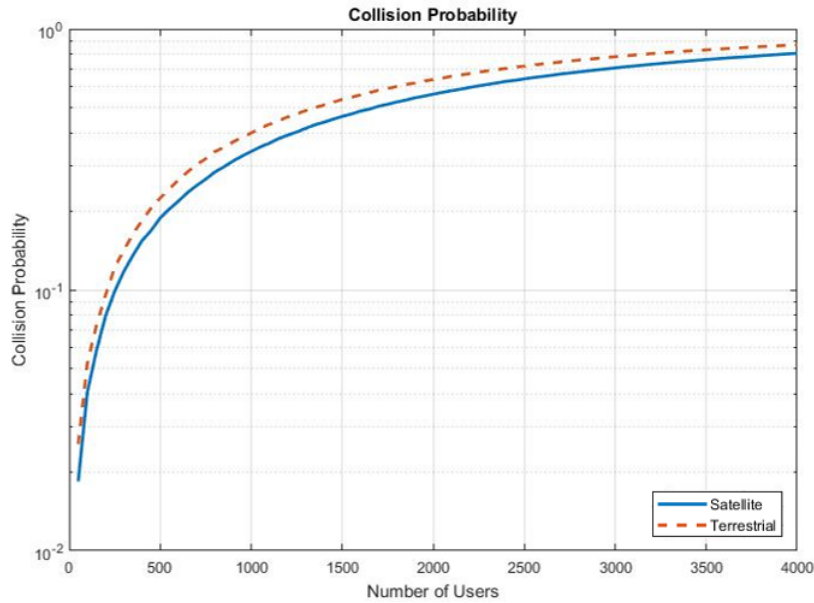


Figure 21: Collision probability comparison between terrestrial and satellite ALOHA.

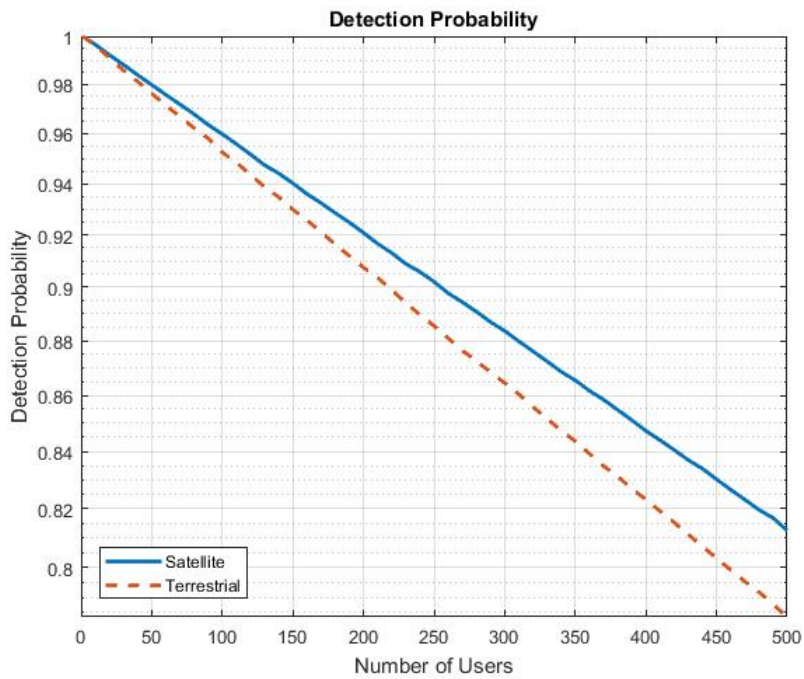


Figure 22: Detection probability comparison between terrestrial and satellite ALOHA.

In both figures, it can be clearly seen that the satellite case has a better performance, which is due to the fact that, thanks to the Doppler effect, packets have a larger area in which to appear, avoiding this way more collisions than in the terrestrial case. It must be mentioned that this

comparison only has taken into account the impact of the Doppler and has proposed an approach to benefit from. To make a thorough comparison other aspects like the link budget, the interferences, the radiation pattern, to mention a few, should be taken into account.

3.4 Conclusions

In this chapter, the ALOHA protocol has been split into four different schemes and its main characteristics have been evaluated as a case of time-frequency access for UNB transmissions. This study has been performed both from a theoretical point of view and results have been confirmed with a strict practical analysis developed with several MATLAB simulations.

It has been concluded that the hybrid cases FUTS and its conjugated case FSTU are the best feasible options, due to the implementation difficulty of the actual best case, the FSTS.

Moreover, it is demonstrated that in a satellite environment, the Doppler effect evaluated on different elevations has not a negative impact on the random-access characteristics, leading to the conclusion that satellite communications are indeed a good option in Low-Power Wide-Area Networks in terms of random access.

Conclusions

This main objective of this project was to study in detail UNB systems as a candidate solution for LPWAN, which are fundamental for the development of concepts such as IoT or M2M. This work has addressed the main objective from two different perspectives, the physical layer and the access layer.

In *chapter 2*, it has been shown that differential BPSK modulation is an excellent option for a UNB communication both for its robustness to phase variations and its acceptable error rate. Moreover, it has been concluded that the best options for shaping pulses in a UNB system are both the MSK pulse with $L=1$ (although its PSD characteristic is not the best, its PAPR behavior is excellent), and the GMSK pulse with $L=4$.

In *chapter 3*, from a theoretical and practical point of view it has been concluded that the hybrid cases for ALOHA protocol, which are FUTS and its conjugated case FSTU are the best options. Moreover, it is demonstrated that in a satellite background, the Doppler effect evaluated on different elevations has not a negative impact on the random-access characteristics, leading to the conclusion that satellite communications are indeed a good option, which is the main contribution of this project to the State of the Art.

In conclusion, it can be stated that UNB systems are indeed a feasible solution for LPWAN, given its positive characteristics both in the physical and MAC layer.

References

- [1] **C. Goursaud, J.M. Gorce, “Dedicated Networks for IoT: PHY / MAC state of the art and Challenges”** in HAL, EAI endorsed transaction on IoT, 2015.
- [2] **J.M. Torres, H. Paz, “Spectral Efficiency and Error Probability Study and Comparison in GMSK and DBPSK modulation schemes”** in Engineering and Investigation Magazine, vol. 28, no 3, pp. 75-80, Dec 2008.
- [3] **P. Laurent, “Exact and Approximate Construction of Digital Phase Modulations by Superposition of Amplitude Modulated Pulses (AMP)”** in IEEE Transactions on Communications, vol. 34, no 2, pp. 150-160, Feb 1986.
- [4] **C. Goursaud, Y. Mo, “Random Unslotted Time-Frequency ALOHA: Theory and Application to IoT UNB Networks”** in 23rd International Conference on Telecommunications, 2016.
- [5] **A. Guidotti, A. Vanelli-Coralli, M.Caus, J.Bas, G. Colavolpe, T. Foggi, S. Cioni, A. Modenini, D. Tarchi, “Satellite-enabled LTE Systems in LEO Constellations”** in Proceedings of 1st International Workshop on Satellite Communications – Challenges and Integration in the 5G ecosystem, May 2017.
- [6] **M. Anteur, V. Deslandes, N. Thomas, A. Beylot, ”Modeling and Performance Analysis of Ultra Narrow Band System for M2M”** in Advanced Satellite Multimedia Systems Conference and the 14th Signal Processing for Space Communications Workshop, Sep 2016.